References

1. Yin YP, Han Y, Dai XQ, Zheng HP, Chen SC, Zhu BY, et al. Susceptibility of *Neisseria gonorrhoeae* to azithromycin and ceftriaxone in China: a retrospective study of national surveillance data from 2013 to 2016. PLoS Med. 2018;15:e1002499. http://dx.doi.org/10.1371/journal.pmed.1002499
2. Chen SC, Yin YP, Chen XS. Cephalosporin-resistant *Neisseria gonorrhoeae* clone, China. Emerg Infect Dis. 2018;24:804–6. http://dx.doi.org/10.3201/eid2404.171817
3. Martin IM, Ison CA, Aanensen DM, Fenton KA, Spratt BG. Rapid sequence-based identification of gonococcal transmission clusters in a large metropolitan area. J Infect Dis. 2004;189: 1497–505. http://dx.doi.org/10.1086/383047
4. Jolley KA, Maiden MC. BIGSdb: Scalable analysis of bacterial genome variation at the population level. BMC Bioinformatics. 2010;11:595. http://dx.doi.org/10.1186/1471-2105-11-595
5. Demczuk W, Sidhu S, Unemo M, Whiley DM, Allen VG, Dillon JR, et al. *Neisseria gonorrhoeae* sequence typing for antimicrobial resistance, a novel antimicrobial resistance multilocus typing scheme for tracking global dissemination of *N. gonorrhoeae* strains. J Clin Microbiol. 2017;55:1454–68. http://dx.doi.org/10.1128/JCM.00100-17
6. Nakayama S, Shimuta K, Furubayashi K, Kawahata T, Unemo M, Ohnishi M. New ceftriaxone- and multidrug-resistant *Neisseria gonorrhoeae* strain with a novel mosaic *penA* gene isolated in Japan. Antimicrob Agents Chemother. 2016;60:4339–41. http://dx.doi.org/10.1128/AAC.00504-16
7. Terkelsen D, Tolstrup J, Johnsen CH, Lund O, Larsen HK, Worning P, et al. Multidrug-resistant *Neisseria gonorrhoeae* infection with ceftriaxone resistance and intermediate resistance to azithromycin, Denmark, 2017. Euro Surveill. 2017;22. http://dx.doi.org/10.2807/1560-7917.ES.2017.22.42.17-00659
8. Lefebvre B, Martin I, Demczuk W, Deshaies L, Michaud S, Labbé AC, et al. Ceftriaxone-resistant *Neisseria gonorrhoeae*, Canada, 2017. Emerg Infect Dis. 2018;24:381–3. http://dx.doi.org/10.3201/eid2402.171756
9. Lahra MM, Martin I, Demczuk W, Jennison AV, Lee KI, Nakayama SI, et al. Cooperative recognition of internationally disseminated ceftriaxone-resistant *Neisseria gonorrhoeae* strain. Emerg Infect Dis. 2018;24:735–40. http://dx.doi.org/10.3201/eid2404.171873
10. Wi T, Lahra MM, Ndowa F, Bala M, Dillon JR, Ramon-Pardo P, et al. Antimicrobial resistance in *Neisseria gonorrhoeae*: Global surveillance and a call for international collaborative action. PLoS Med. 2017;14:e1002344. http://dx.doi.org/10.1371/journal.pmed.1002344

Address for correspondence: Yue-Ping Yin, National Center for STD Control, China CDC—Reference Laboratory, 12 Jiangwangmiao St, Nanjing, Jiangsu 210042 China; email: yinyp@ncstdlc.org

Disseminated Metacestode *Versteria* Species Infection in Woman, Pennsylvania, USA[1]

Bethany Lehman, Sixto M. Leal, Jr., Gary W. Procop, Elise O'Connell, Jahangheer Shaik, Theodore E. Nash, Thomas B. Nutman, Stephen Jones, Stephanie Braunthal, Shetal N. Shah, Michael W. Cruise, Sanjay Mukhopadhyay, Jona Banzon

Author affiliations: Cleveland Clinic Foundation, Cleveland, Ohio, USA (B. Lehman, G.W. Procop, S. Jones, S. Braunthal, S.N. Shah, M.W. Cruise, S. Mukhopadhyay, J. Banzon); University of Alabama Medical Center, Tuscaloosa, Alabama, USA (S.M. Leal, Jr.); National Institutes of Health, Bethesda, Maryland, USA (E. O'Connell, J. Shaik, T.E. Nash, T.B. Nutman)

DOI: https://doi.org/10.3201/eid2507.190223

A patient in Pennsylvania, USA, with common variable immunodeficiency sought care for fever, cough, and abdominal pain. Imaging revealed lesions involving multiple organs. Liver resection demonstrated necrotizing granulomas, recognizable tegument, and calcareous corpuscles indicative of an invasive cestode infection. Sequencing revealed 98% identity to a *Versteria* species of cestode found in mink.

In July 2017, a 68-year-old woman in Pennsylvania, USA, sought care for fever, fatigue, cough, and abdominal pain. Her medical history was significant for common variable immunodeficiency and splenic B cell lymphoma that had been treated with R-CHOP (rituximab, cyclophosphamide, hydroxydaunorubicin, vincristine, and prednisone); treatment was completed in December 2016.

Imaging showed extensive nodular disease of the lungs and liver and a hepatic abscess. Examination of a fine-needle aspirate of the hepatic lesion detected hepatocytes with focal atypia on a background of marked acute inflammation and necrosis, suggestive of an active infectious process. Subsequent percutaneous needle biopsy samples of the liver, bronchoalveolar lavage and transbronchial biopsy samples, and surgical biopsy samples of the left lower lobe showed necrotizing granulomas and reactive/reparative tissue changes. All histochemically stained slides (Gomori-methenamine silver, Gram, periodic acid Schiff, Warthin-Starry, Ziehl-Neelsen, Fite) yielded negative results for microorganisms. Results of broad-range PCR for bacteria

[1]This manuscript was originally presented at the Infectious Disease Society of America IDWeek 2018; October 3–7, 2018; San Francisco, CA, USA.

(16S rDNA), fungi (28S rDNA), and mycobacteria (16S rDNA, *rpo*B, and *hsp*65) were also negative.

Four months later, after the patient had been receiving broad-spectrum antibacterial and antifungal medications, she sought a second opinion at the Cleveland Clinic (Cleveland, OH, USA), where repeat cross-sectional imaging showed progressive nodular disease within the lungs, liver, and kidneys and cyst-like lesions in the eyes and brain (Appendix Figure 1, https://wwwnc.cdc.gov/EID/article/25/7/19-0223-App1.pdf). Gross examination of a liver sample from a right partial hepatectomy performed for diagnosis revealed multifocal tan-white nodules and necrotic or cystic spaces. Microscopic analysis identified extensive necrotizing granulomatous inflammation and multifocal cystic spaces, which enclosed material characteristic of the tegument of a cestode. In a separate location within otherwise nondescript necrotic tissue was a focal collection of round basophilic concretions with concentric layers of deposited material characteristic of calcareous corpuscles, pathognomonic for a cestode infection (Appendix Figure 2). Additional histochemical studies for microorganisms detected no microorganisms.

These findings were consistent with a disseminated proliferating invasive cestode infection; the metacestode most closely resembled the cysticercus larva that lacks a scolex (i.e., the racemose form of cysticercosis). The presence of racemose-like disseminated involvement of multiple visceral organs was concerning because this feature is not common in patients with cysticercosis. Results of an enzyme-linked immunotransfer blot for *Taenia solium* cestodes were negative. Cysticercus-specific IgG was not elevated, and antibodies against echinococci were not found, although these tests are unreliable in a patient who has common variable immunodeficiency and is receiving intravenous immunoglobulin. Therefore, we considered the possibility of another cestode species.

The patient received praziquantel and albendazole for 1 month. Initially, dexamethasone (10 mg) was concurrently administered for the neurologic and ocular involvement. Treatment resolved the abdominal pain, fatigue, and fever. Follow-up imaging showed vast improvement in the brain, lung, kidney, and liver lesions. Imaging findings continued to improve after corticosteroids were tapered off after 3 months, and symptoms continued to improve 6 months after treatment. However, serial eye examinations revealed a new cystic lesion in the eye. The cyst was extracted; histopathologic examination did not detect a scolex but did detect an identical tegument, again appearing as an aberrant form (Appendix Figure 2). As of April 2019, the patient was continuing to receive albendazole and praziquantel and monthly intravenous immunoglobulin.

Because of the unusual histopathologic findings and clinical course, we performed molecular analysis. We extracted DNA from formalin-fixed, paraffin-embedded liver tissue and then performed partial mitochondrial

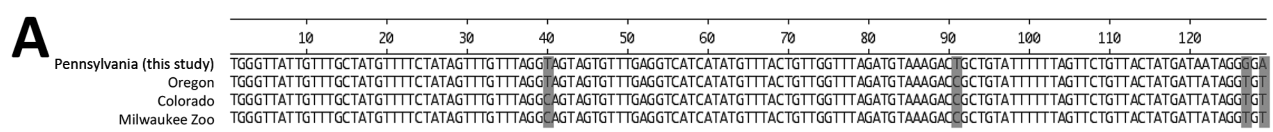

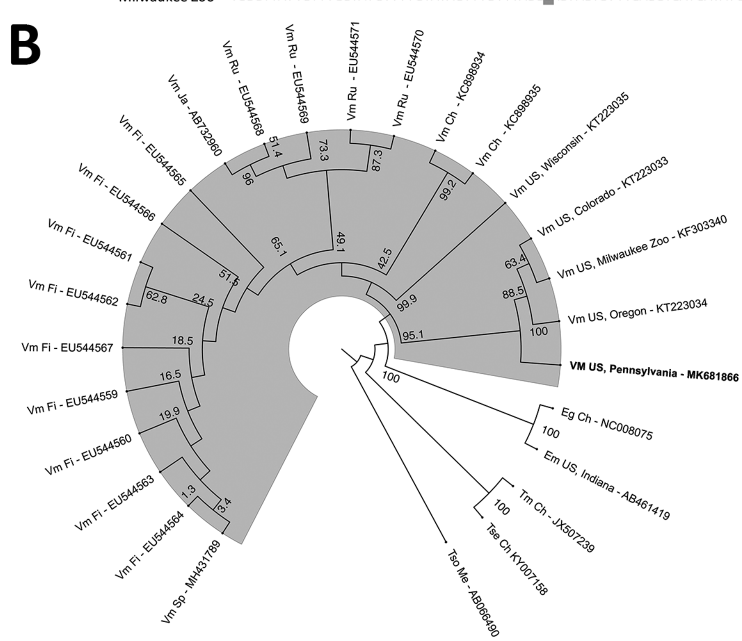

Figure. Test results for woman with disseminated *Versteria* sp. cestode infection, Pennsylvania, USA. A) Sequence of the 129-bp fragment of cytochrome c oxidase subunit 1 (*cox1*) gene from patient compared with 3 closely related *Versteria* sp. isolates from the United States. Shading indicates differing nucleotides. B) Phylogenetic tree based on the *cox1* gene of all reported Vm *cox1* sequences with country of origin and other clinically relevant cestodes; GenBank accession numbers are provided. Boldface indicates the Vm sequence reported in this study; shading represents the outbranching of Vm. Bootstrap values are shown. Ch, China; Eg, *Echinococcus granulosus*; Em, *Echinococcus multilocularis*; Fi, Finland; Ja, Japan; Me, Mexico; Ru, Russia; Sp, Spain; Tm, *Taenia multiceps*; Tse, *T. serialis*; Tso, *T. solium*; US, United States; Vm, *Versteria* sp. mitochondrial.

cytochrome (*cox1*) gene amplification. (*1*). PCR products were inserted into pCR 2.1 TOPO (https://www.thermofisher.com), cloned, and sequenced (at Macrogen USA, Rockville, MD, USA; https://www.macrogenusa.com). Our search for a 128-bp consensus sequence by using BLAST (https://blast.ncbi.nlm.nih.gov/Blast.cgi) found a 98% match to the *Versteria* species *cox1* gene (GenBank accession no. KT223034). After disease recurrence and soon after extraction of the ocular cyst, we subsequently subjected DNA from the preserved ocular cyst to Nanopore sequencing (Oxford Nanopore Technologies, https://nanoporetech.com) and assembled the complete mitochondrial genome, which we deposited at GenBank (accession no. MK681866) (Figure).

The definitive hosts of the new *Versteria* (*Taenia mustelae*) cestodes are usually mustelids (*2*), a family of carnivorous mammals including weasels, ermine, mink, and others, which are found throughout the northern United States (*3*). This patient reported exposure to fishers in her residence in western Pennsylvania, where a resurgence in the population of these members of the family Mustelidae has been observed. Her husband was screened for signs of a parasitic infection and results were negative. The only other reported human infection with *Versteria* sp. involved a kidney transplant patient, who also had lung and liver lesions. Histopathologic examination of that patient's liver lesions revealed focal necrotizing granulomas with hooklets and a protoscolex (*4*).

The diagnosis of a cestode infection is usually suggested by the presence of specific cestode structures (e.g., a protoscolex, tegument, or calcareous corpuscles). However, unlike the previous report of human infection, histopathologic examination of the liver lesion and ocular cyst from this patient did not detect hooklets or protoscoleces, mimicking the histopathologic appearance of racemose disease sometimes seen in patients with subarachnoid neurocysticercosis. Because histopathologic examination is insufficient for species-level identification (specific cestode structures), molecular testing is necessary for definitive diagnosis of *Versteria* sp. cestode infection.

Acknowledgments
We thank Kevin El-Hayek, who performed the liver biopsy, and Sunil Srivastava for the fundus photograph.

This study was partially funded through the Division of Intramural Research, National Institute of Allergy and Infectious Disease, National Institutes of Health.

About the Author
Dr. Lehman is an infectious disease physician at the Cleveland Clinic. Her primary research interest is osteoarticular infections.

References
1. Poon RWS, Tam EWT, Lau SKP, Cheng VCC, Yuen KY, Schuster RK, et al. Molecular identification of cestodes and nematodes by *cox1* gene real-time PCR and sequencing. Diagn Microbiol Infect Dis. 2017;89:185–90. http://dx.doi.org/10.1016/j.diagmicrobio.2017.07.012
2. Lee LM, Wallace RS, Clyde VL, Gendron-Fitzpatrick A, Sibley SD, Stuchin M, et al. Definitive hosts of *Versteria* tapeworms (Cestoda: Taeniidae) causing fatal infection in North America. Emerg Infect Dis. 2016;22:707–10. http://dx.doi.org/10.3201/eid2204.151446
3. Bininda-Emonds OR, Gittleman JL, Purvis A. Building large trees by combining phylogenetic information: a complete phylogeny of the extant Carnivora (Mammalia). Biol Rev Camb Philos Soc. 1999;74:143–75. http://dx.doi.org/10.1017/S0006323199005307
4. Barkati S, Gottstein B, Mü Ller N, Sheitoyan-Pesant C, Metrakos P, Chen T, et al. First human case of metacestode infection caused by *Versteria* sp. in a kidney transplant recipient. Clin Infect Dis. 2019;68:680–3. http://dx.doi.org/10.1093/cid/ciy602

Address for correspondence: Bethany Lehman, Cleveland Clinic, Department of Infectious Disease, 9500 Euclid Ave/G21, Cleveland, OH 44195, USA; email: lehmanb@ccf.org

Increased Threat of Urban Malaria from *Anopheles stephensi* Mosquitoes, Africa

Willlem Takken, Steve Lindsay

Author affiliations: Wageningen University & Research, Wageningen, the Netherlands (W. Takken); Durham University, Durham, UK (S. Lindsay)

DOI: https://doi.org/10.3201/eid2507.190301

Malaria continues to be a major health threat in Africa, mainly in rural areas. Recently, the urban malaria vector *Anopheles stephensi* invaded Djibouti and Ethiopia, potentially spreading to other areas of Africa. Urgent action is needed to prevent urban malaria epidemics from emerging and causing a public health disaster.

The pernicious life-threatening disease malaria continues to place a heavy burden on communities in Africa, where >92% of malaria cases occur today (*1*). Mosquitoes of the genus *Anopheles* transmit malaria parasites to humans. Africa has ≥128 indigenous *Anopheles* species (*2*), several of which, *An. gambiae sensu stricto*, *An. coluzzii*,

Article DOI: https://doi.org/10.3201/eid2507.190223

Disseminated *Versteria* Sp. Metacestode Infection in Woman, Pennsylvania, USA

Appendix

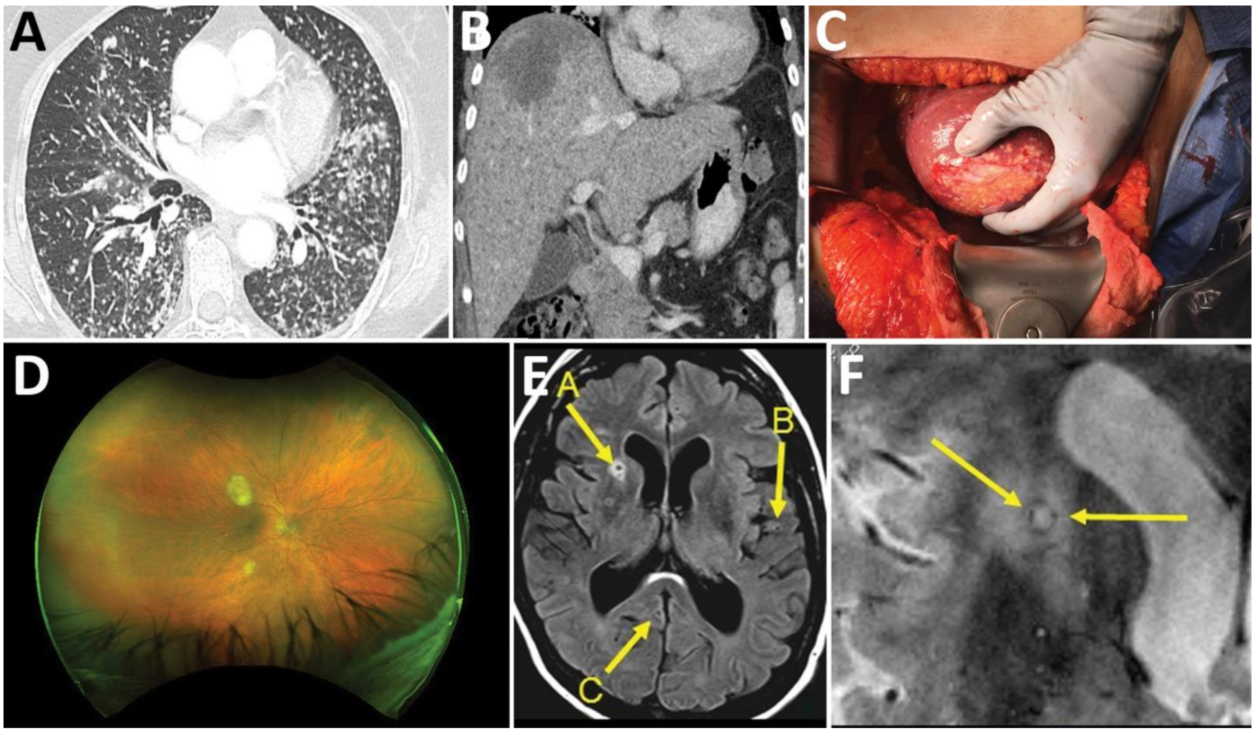

Appendix Figure 1. Images of patient with *Versteria* sp. infection. A) Contrast-enhanced CT scan of the chest showing numerous randomly distributed sub-centimeter nodules throughout both lungs with predominant involvement in mid to lower lungs. B) Coronal reformatted image from contrast enhanced CT scan of the abdomen demonstrating a low attenuation right hepatic dome lesion measuring 6.0 × 4.7 cm, numerous smaller low attenuation lesions in the liver. C) Visualization of the liver at surgery revealing multifocal tan-white nodules and cystic spaces. D) Wide field fundus photo which reveals 2 oval subretinal lesions in the right eye. E) Axial FLAIR image from 7T MRI, showing three example cystic lesions: (A) right anterior limb of the internal capsule; (B) left temporal operculum; and (C) right posterior cingulate gyrus. Lesion A demonstrates mild peri-lesional edema. Numerous other lesions were found throughout the brain (not shown). F) Magnified view of lesion A in 1e, using a high resolution T2* GRE sequence, showing voids (dark signal) at lesions periphery representing calcification or iron in the wall of the lesion.

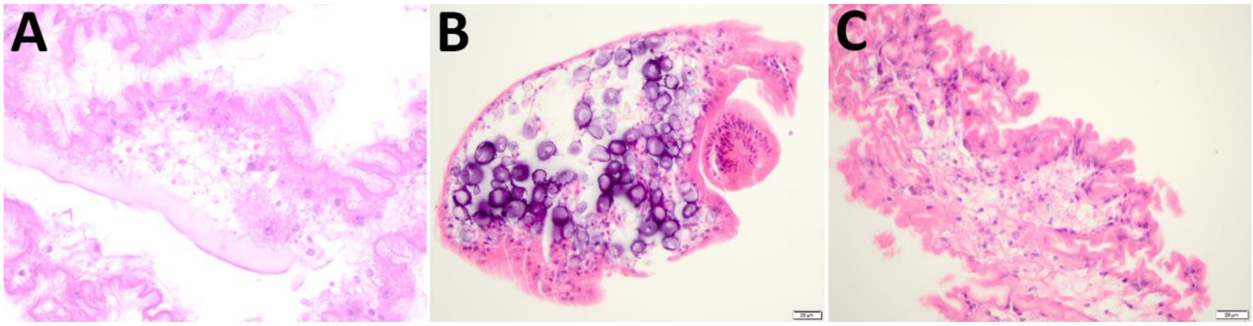

Appendix Figure 2. Histopathology images of tissue from patient with *Versteria* sp. infection. A) Degenerating three-layered membrane characterized by a undulating, eosinophilic outer cell layer with microvilli underlying degenerating cells with pyknotic nuclei (i.e., pyknotic cell layer), and degenerating loose connective tissue from the open liver biopsy. B) Numerous calcareous corpuscles (ie purple structures) and protoscolex obtained from the ocular cyst extraction. C) Ocular cyst demonstrating the three-layered membrane again with outer layer with microvilli, pyknotic cell layer and loose connective tissue.